3D Characterization of Underfoliage Targets Using L-band To- mographic SAR Data and A Wavelet-Based Approach

Yue Huang, Jacques Lévy Véhel, Laurent Ferro-Famil, Andreas Reigber, Stefano Fortunati

3D Characterization of Underfoliage Targets Using L-band Tomographic SAR Data and A Wavelet-Based Approach

Yue Huang, INRIA, yue.huang@inria.fr, France
Jacques Levy-Vehel, INRIA, France
Laurent Ferro-Famil, University of Rennes 1, France
Andreas Reigber, Microwaves and Radar Institute, German Aerospace Center (DLR), Germany
Stefano Fortunati, University of Pisa, Italy.

Abstract

SAR imaging of underfoliage targets has to face a complex mixture of diverse scattering mechanisms. To characterize this complex scattering environment, nonparametric tomographic estimators are more robust to focusing artefacts but limited in resolution. Parametric tomographic estimators provide better vertical resolution but fail to adequately characterize continuously distributed volumetric scatterers such as forest canopies. To overcome these limitations, this paper addresses a new wavelet-based approach for 3D characterization of underfoliage targets. The effectiveness of this new approach is demonstrated by using L-band Multi-Baseline PolInSAR Data over Dornstetten, Germany.

1 Introduction

Hybrid environments refer to a scenario of objects embedded in a host natural environment (e.g. forests). Their scattering patterns consist of a complex mixture of diverse scattering mechanisms, like the volume scattering from the canopy, double bounce reflection between the ground and under-foliage objects as well as between an object and trunks, surface scattering from the underlying ground, etc. The resulting SAR information is characterized by a strong complexity, which makes SAR image analysis difficult by means of PolInSAR data (due to the single-baseline configuration). Multi-baseline PolInSAR techniques can be applied to reconstruct the associated scattering responses and polarimetric patterns. In [1], using single polarization tomograms, the forest profile and truck shape were both extracted using Capon's spectral estimation approach. However, due to the limited spectral resolution and sidelobe suppression of such an approach, parametric and fully polarimetric tomographic approaches are expected to show significantly improved features of under-foliage objects and forests as it has been shown in [2]. In [1, 2], the applied spectral estimation methods are either nonparametric or parametric. It is known that nonparametric approaches are in general more robust to focusing artefacts, whereas parametric approaches are characterized by a better vertical resolution. It has been shown [3, 4] that the performance of these spectral analysis approaches is conditioned by the nature of the scattering response of the observed objects.

The scattering power from forest canopy in elevation can be characterized by continuous spectrum, since volumic scatterers are continuously distributed in vertical. Scattering responses from the objects or ground are considered to be localized discretely in the vertical direction. The under-foliage object with a deterministic scattering response embedded in the surrounding distributed environments, should be characterized by a mixed spectrum. Considering Conventional tomographic estimators, either nonparametric methods(e.g.Capon, Beamforming) or parametric methods (e.g. Maximum likelihood)are limited to one type of spectrum or the other, due to the lack of adaptation to the mixed spectrum. Semiparametric methods like sparse estimation methods, have been used for compressive sensing over urban areas in [5] and over forested areas in [6]. However for this scenario of complex mixed scattering environment, a new wavelet-based approach is proposed, adapted to characterize the hybrid nature of the observed environment. The effectiveness of the proposed method is demonstrated by using the L-band multibaseline InSAR data acquired over the test site of Dornstetten, Germany.

2 Tomographic Signal Model

The MB-InSAR configuration consists of M acquisition positions, each pair of which are separated by a baseline. Considering an azimuth-range resolution cell that contains K backscattering contributions from scatterers located at different heights $\mathbf{z} = [z_1, \ldots, z_K]$, the received data vector, $\mathbf{y} \in \mathbb{C}^{M\times 1}$, can be formulated as follows:

$$\mathbf{y}(l) = \sum_{i=1}^{K} \mathbf{a}(z_i) s_i(l) + \mathbf{n}(l) \qquad (1)$$

where $l = 1, \ldots, L$ indicates one of the L independent realizations of the signal acquisition. The complex additive noise $\mathbf{n} \in \mathbb{C}^M$ is assumed to be Gaussianly distributed with zero mean and variance σ_n^2 and to be white in time and space. The steering vector $\mathbf{a}(z)$ contains the interferometric phase information associated to a source located at the elevation position z above the reference focusing plane and is given by:

$$\mathbf{a}(z) = [1, \exp(jk_{z_2} z), \ldots, \exp(jk_{z_M} z)]^T \qquad (2)$$

where $k_{z_j} = \frac{4\pi}{\lambda} \frac{B_{\perp_j}}{r_1 \sin\theta}$ is the two-way vertical wavenumber between the master and the jth acquisition tracks.

The carrier wavelength is represented by λ, whereas θ stands for the incidence angle and r_1 is the slant range distance between the master track and the scatterer. As k_{z_j} is calculated from acquisition system parameters, $\mathbf{a}(.)$ is a known function but the source elevation z is unknown. The source signal vector, $\mathbf{s} = [s_1 \dots s_K] \in \mathbb{C}^K$, contains the unknown complex backscattering coefficients of the K source scatterers. We are interested in recovering the power distribution in elevation (i.e. tomographic profile), $\mathbf{x} = [|s_1|^2, \dots, |s_K|^2] \in \mathbb{R}^K$, from the observed data $[\mathbf{y}(1), \dots \mathbf{y}(L)] \in \mathbb{C}^{M \times L}$. Conventionally, $K < M$ scatterers are assumed to be located within one resolution cell. However, the forest canopy consists of a large number of elementary scatterers continuously distributed in the vertical direction. To characterize the object embedded in a forest environment, it is reasonable to assume $K >> M$. In order to solve this underdetermined problem, a wavelet-based sparse estimation method is proposed in the following section.

3 Tomographic Estimation

In the frame of urban remote sensing, the l_1 norm regularization has been used for tomographic SAR inversion by [5]. This compressive approach can efficiently localize the point-like scatterers in the vertical direction, but can not directly deal with volumic media because the volumic scatterers are not distributed sparsely in the vertical domain. In [6], a wavelet-based compressed sensing technique has been developed for SAR tomography of forested areas and it provided undeniable performance for forest characterization. However this approach lacks high resolution to characterize the objects beneath the canopy. For this purpose, a criterion is proposed and compactly written in a standard format of l_1 norm minimization with quadratic constraints

$$\min_{\mathbf{x}} ||\mathbf{B}\mathbf{x}||_1 \text{ subject to } \quad ||\mathbf{A}\mathbf{\Lambda}_{\mathbf{x}}\mathbf{A}^\dagger - \widehat{\mathbf{R}}||_F \leq \epsilon \tag{3}$$

where

- $\mathbf{x} = \begin{bmatrix} \mathbf{x}_1 \\ \mathbf{x}_2 \end{bmatrix} \in \mathbb{R}^K$: scattering power distribution in elevation. $\mathbf{x}_1 \in \mathbb{R}^p$ and $\mathbf{x}_2 \in \mathbb{R}^q$ represent respectively scattering power distribution for the objects and canopy in elevation ($N = p + q$).
- $\mathbf{B}\mathbf{x} = \begin{bmatrix} \mathbf{I}_{(p\times p)} & \mathbf{0} \\ \mathbf{0} & \mathbf{\Psi} \end{bmatrix} \mathbf{x} = \begin{bmatrix} \mathbf{x}_1 \\ \mathbf{\Psi}\mathbf{x}_2 \end{bmatrix} \in \mathbb{R}^K$: sparse signal.
  - $\mathbf{x}_1 \in \mathbb{R}^p$ is sparse as the scattering responses of an object may be described with a few scatterers discretely localized in elevation.
  - $\mathbf{\Psi}\mathbf{x}_2 \in \mathbb{R}^q$ represents the projection of canopy power distribution $\mathbf{x}_2$ onto an orthonormal wavelet basis $\mathbf{\Psi} \in \mathbb{R}^{q\times q}$. The power distribution of canopy in elevation, $\mathbf{x}_2$, depicts continuous regular signal behaviors, so its projection onto wavelet basis, $\mathbf{\Psi}\mathbf{x}_2$, is sparse.
- $\mathbf{\Lambda}_{\mathbf{x}} = diag(\mathbf{x}) \in \mathbb{R}^{N\times N}$.
- $\widehat{\mathbf{R}} = \frac{1}{L}\sum_1^L \mathbf{y}(l)\mathbf{y}^\dagger(l) \in \mathbb{R}^{M\times M}$: sample covariance matrix of observed data.
- ϵ: tolerance parameter to control model mismatch and signal sparsity.

By minimizing the criterion (3), the solution $\widehat{\mathbf{x}}$ is obtained that reconstructs the vertical power distribution of underfoliage objects. In practice, the problem in (3) is under SOCP formulation and can be solved by any convex optimization solver proposed in the field of sparse recovery estimation. In this paper, the CVX solver is implemented to solve this standard l_1 norm minimization, due to its implementation facility and compactness. The parameter ϵ is selected based on noise variance σ_n^2, so according the (3), ϵ should be $\propto \sqrt{M}\sigma_n^2$, e.g. for our applied data sets, we choose ϵ=$4\sqrt{M}\sigma_n^2$.

For the sparse estimation controlled by the user-selected parameter, the drawback is the source signal power leaks into the neighboring sampling intervals. This fact may be due to the inappropriate choice for the parameter ϵ. If ϵ is chosen too small, then the measured data will be overfitted and the mainlobe of the source signal power spectrum may be splitted in several peaks, especially in the low SNR case. The other reason may be due to the off-grids effects and basis mismatch[7],[8]. This type of leakage happens more often to the estimated signal associated to the $\mathbf{I}$ basis, i.e. $\mathbf{x}_1$ in our criterion (3) . To solve this issue, a merging processing based on linear interpolation is used here, similar as in [7]. Candidate peaks with amplitude $> \max(|\widehat{\mathbf{x}}_1|)/10$ can be selected from estimated reflectivity $\widehat{\mathbf{x}}_1$ for underfoliage objects or ground reflection. Taking a window with width Δ and centering at each peak location z_i, the neighboring peaks $[z_{i_1}, \dots, z_{i_d}]$ located within $[z_i - \Delta/2, z_i + \Delta/2]$ are merged in such a way: $z_m = z_{ic} + \sum_{k=1}^d \mathbf{x}_1(z_i)(z_{i_k} - z_{ic}) / \sum_{k=1}^d \mathbf{x}_1(z_i)$ with $z_{ic} = (z_{i_1} + \dots + z_{i_d})/d$. This method effectively merges splitted peaks within a filtering window Δ into one peak.

4 Experimental Results

The tomographic analysis of a volumetric forested area and sub-canopy objects is led using polarimetic L-band airborne data acquired by the DLR's E-SAR system over the Dornstetten test site, Germany. The acquisition geometry consists of 23 flight tracks, three of which are located very close to each other (quasi-null spatial baseline) in order to estimate the temporal decorrelation. Thus 21 tracks are effectively used for the tomographic analysis. The horizontal baselines form a quasi-uniform linear array with an average baseline close to 20 m and the geometric vertical resolution is about 2 m. This quasi-regular distribution provides 3D features with reduced sidelobe levels and hence facilitates the tomographic analysis. The test zone for underfoliage objects is shown in Fig.1.

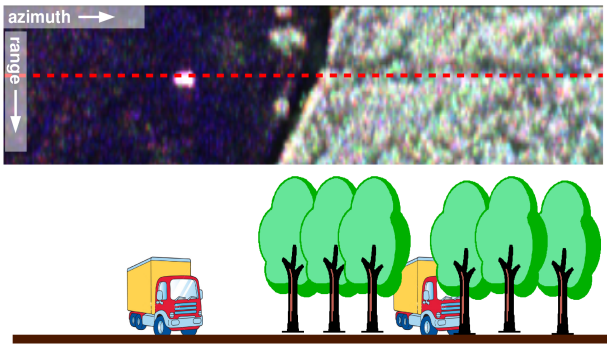

Figure 1: Pauli image for test area where trucks are set

4.1 Vertical reflectivity profiles

The wavelet basis Φ should be selected based on the criterion that the coherence between the measurement matrix $\mathbf{A}$ and wavelet basis Φ should be as small as possible. More details of the wavelet basis selection have been provided in [6]. The sym4 wavelet with 3-level decomposition has been used to form Φ in [6] which shows excellent performances for the reflectivity recovery of forests in vertical direction. Due to the same test data set used in this paper, we keep the same choice for wavelet basis Φ.

Considering firstly the simple scenarios in this test areas, the recovered scattering profiles from HH channel are shown in Fig.2(a)-(c). The reflectivity profile, $\mathbf{x}$, directly estimated from (3) (in blue) may produce splitted peaks, e.g. over the bare soil in Fig.2(a). The reflectivity profile after merging is shown in black. Clearly depicted in Fig.2(a), the merging processing effectively merges the closely-spaced neighboring peaks into a single one and its interpolated location coincides with Beamforming or Capon estimation.

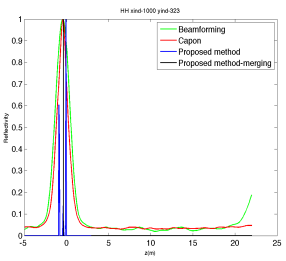

(a) Soil-HH

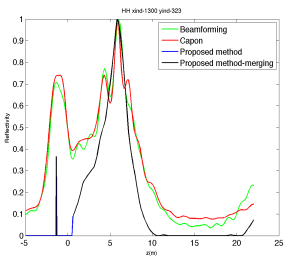

(b) Forest-HH

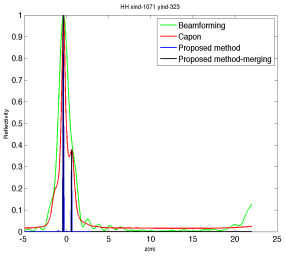

(c) Uncovered Truck-HH

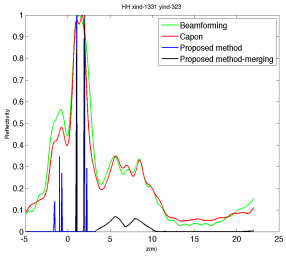

(d) Covered Truck-HH

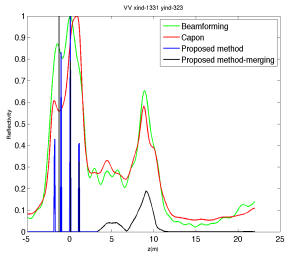

(e) Covered Truck-VV

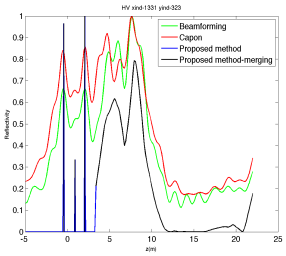

(f) Covered Truck-HV

Figure 2: Normalized scattering power distribution in elevation for underfoliage truck using different polarimetric data sets. Horizontal axis: height z(m). Vertical axis: normalized scattering power.

Applying now the proposed wavelet-based approach to a pixel related to the underfoliage object, the reflectivity function is estimated along elevation shown Fig.2 (d)-(f). Compared with Capon (green) and Beamforming (red) methods, the new estimation method provides much better resolution than conventional non-parametric methods for the underfoliage object. The estimated height for the covered truck is around 3m, validated with the ground truth. For the vertical profile of forest canopy, the reflectivity seems underestimated by the proposed method compared with Capon and Beamforming methods. Two reasons may be considered. One reason is the leakage of canopy backscattering power into the underfoliage space. The second reason is more postive: the proposed method gives a clean or denoised version of the estimated reflectivity. Looking into the power spectra of Capon and Beamforming methods, the noise power around the elevation boundaries, i.e. close to -5m and 22m, is not fully attenuated.

4.2 Tomograms of the test line

The entire test line is estimated by diverse tomographic estimators and the resulting reflectivity tomograms are given in Fig.3. The Capon tomogram depicts trucks with a poor vertical resolution due to the nature of continuous spectrum (Fig.3(a)), although it can well charcterize the forest canopy. Using n_s estimated by diagonal loading MOS technique in [9], the MUSIC tomogram characterizes the uncovered truck with strong sidelobes in the vertical direction and the forests with a limited number of scatterers (Fig.3(b)). Moreover, the underfoliage trucks are not visibly shown in the above two tomograms. Applying now the proposed wavelet-based method and merging process, the resulting tomogram demonstrates the continuous spectrum for the canopy and the high-resolution discrete spectrum for the ground and underfoliage object as shown in Fig.3(c). Also using the proposed method, the ground and underfoliage scattering power can be separated from the distributed scattering of canopy and their tomograms can be respectively shown in Fig.3(d) and (e).

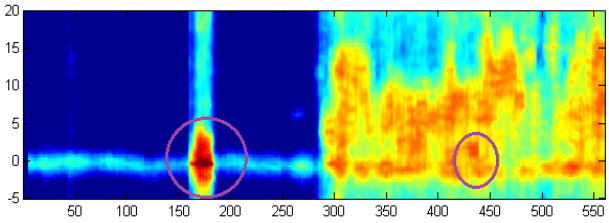

(a) Capon

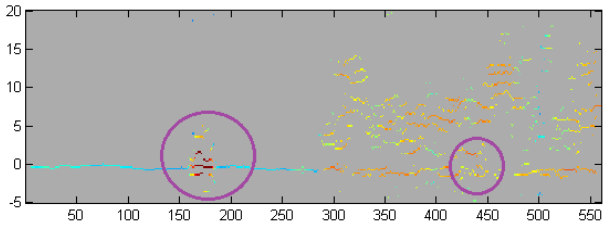

(b) MUSIC

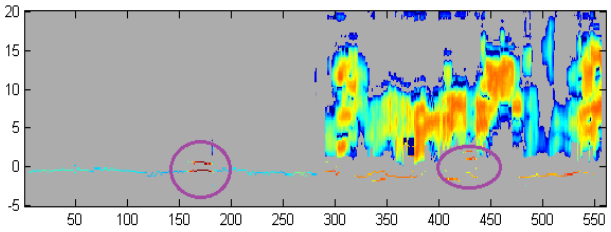

(c) Proposed method with merging

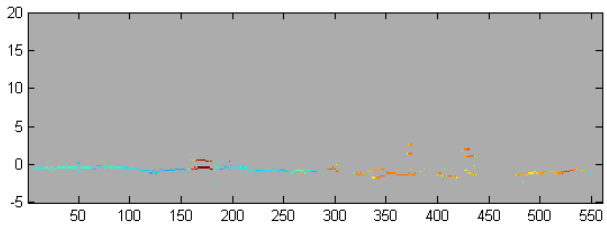

(d) Ground and underfoliage scattering ($\mathbf{x}_1$) estimated by proposed method with merging

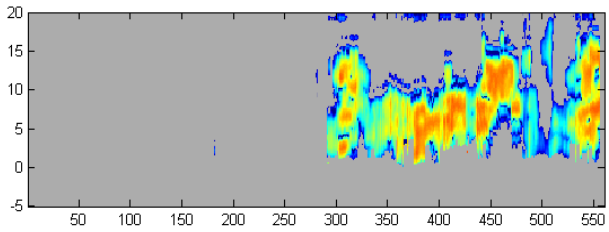

(e) Canopy power ($\mathbf{x}_2$) estimated by proposed method with merging

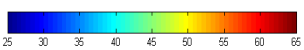

(f) dB

Figure 3: Reflectivity tomograms estimated by the proposed method with merging processing using HH data set. (Gray background:zero reflectivity).

References

[1] M.Nannini, R.Scheiber, and R.Horn. Imaging of targets beneath foliage with sar tomography. *Proc. EUSAR*, pages 1–4, June 2008.

[2] Y. Huang, L. Ferro-Famil, and C. Lardeux. Polarimetric sar tomography of tropical forests at p and l-band. *Proc. IGARSS*, pages 1373–1376, July 2011.

[3] P. Stoica and A. Nehorai. Performance study of conditional and unconditional direction-of-arrival estimation. *IEEE Trans. Acoust. Speech Signal Processing*, ASSP-38:1783–1795, Oct 1990.

[4] Y.Huang and L. Ferro-Famil. Building height estimation using multibaseline l-band sar data and polarimetric weighted subspace fitting methods. *Polinsar proceeding*, 2009.

[5] X. X. Zhu and R. Bamler. Tomographic sar inversion by l1 -norm regularization-the compressive sensing approach. *IEEE Transactions on Geoscience and Remote Sensing*, 48(10):3839–3846, Oct 2010.

[6] E. Aguilera, M. Nannini, and A. Reigber. Wavelet-based compressed sensing for sar tomography of forested areas. *Geoscience and Remote Sensing, IEEE Transactions on*, 51(12):5283–5295, Dec 2013.

[7] Z. Tan, P. Yang, and A. Nehorai. Joint-sparse recovery in compressed sensing with dictionary mismatch. *Computational Advances in Multi-Sensor Adaptive Processing (CAMSAP), 2013 IEEE 5th International Workshop on*, pages 248–251, Dec 2013.

[8] S.Xing, D. Dai, Y. Li, and X. Wang. Polarimetric sar tomography using l2,1 mixed norm sparse reconstruction method. *Progress In Electromagnetics Research*, 130:105–130, 2012.

[9] Y. Huang, L. Ferro-Famil, and A. Reigber. Underfoliage object imaging using sar tomography and polarimetric spectral estimators. *IEEE Transactions on Geoscience and Remote Sensing*, 50(6):2213–2225, June 2012.